

C.W. HUANG^{1,2}, J.J. TSAI¹, C.C. HUANG^{2,3}, S.N. WU^{4,5}

EXPERIMENTAL AND SIMULATION STUDIES ON THE MECHANISMS OF LEVETIRACETAM-MEDIATED INHIBITION OF DELAYED-RECTIFIER POTASSIUM CURRENT (K_V3.1): CONTRIBUTION TO THE FIRING OF ACTION POTENTIALS

¹Department of Neurology, National Cheng Kung University School of Medicine, Tainan, Taiwan; ²Institute of Clinical Medicine, National Cheng Kung University School of Medicine, Tainan, Taiwan; ³Department of Pediatrics, National Cheng Kung University School of Medicine, Tainan, Taiwan; ⁴Department of Physiology, National Cheng Kung University School of Medicine, Tainan, Taiwan; ⁵Institute of Basic Medicine, National Cheng Kung University School of Medicine, Tainan, Taiwan

Levetiracetam (LEV) is an S-enantiomer pyrrolidone derivative with established antiepileptic efficacy in generalized epilepsy and partial epilepsy. However, its effects on ion currents and membrane potential remain largely unclear. We investigated the effect of LEV on differentiated NG108-15 neurons. In these cells treated with dibutyryl cyclic AMP, the expression level of the K_v3.1 mRNA was elevated. With the aid of patch clamp technology, we found that LEV could suppress the amplitude of delayed rectifier K⁺ current ($I_{K(DR)}$) in a concentration-dependent manner with an IC₅₀ value of 37 μ M. LEV (30 μ M) shifted the steady-state activation of $I_{K(DR)}$ to a more positive potential by 10 mV, without shifting the steady-state inactivation of $I_{K(DR)}$. Neither Na⁺, nor *erg* (*ether-a-go-go*-related)-mediated K⁺ and ATP-sensitive K⁺ currents were affected by LEV (100 μ M). LEV increased the duration of action potentials in current clamp configuration. Simulation studies in a modified Hodgkin-Huxley neuron and network unraveled that the reduction of slowly inactivating $I_{K(DR)}$ resulted in membrane depolarization accompanied by termination of the firing of action potentials in a stochastic manner. Therefore, the inhibitory effects on slowly inactivating $I_{K(DR)}$ (K_v3.1-encoded current) may constitute one of the underlying mechanisms through which LEV affect neuronal activity *in vivo*.

Key words: *levetiracetam, delayed rectifier K⁺ current, Na⁺ current, action potential, differentiated NG108-15 cell, simulation*

INTRODUCTION

Levetiracetam (LEV, (S)- α -ethyl-2-oxo-pyrrolidine acetamide), a newer antiepileptic drug (AED), has been recognized in combination with other AEDs to treat a variety of seizures in people with epilepsy, including idiopathic generalized epilepsy and refractory partial-onset seizures. (1–4). Previous work showed that LEV could suppress epileptiform discharges induced by bicuculline, whereas it did not inhibit spontaneous sharp potentials and burst discharges elicited by omission of Mg²⁺ from the bath medium (5). Several studies have demonstrated that the binding of LEV to the SV2A presynaptic vesicle protein is an important mechanism through which neuronal excitability is regulated (6–7). However, there are other studies showing that this drug may also have effects on ion currents. For example, LEV could selectively block N-type calcium channels (8). Another report suggested the inhibition of voltage-operated potassium current by LEV, as an antiepileptic mechanism (9). Nevertheless, the comprehensive effects of LEV on ion channels and membrane potential, as a major research interest in antiepileptic drugs, remain not completely understood.

Piracetam, a pyrrolidone derivative structurally related to LEV (10), widely used as a cognitive enhancer, had little or no effect on

$I_{K(DR)}$ in isolated neurons (11). In addition, piracetam was recently reported to suppress the slowly inactivating $I_{K(DR)}$ and Ca²⁺-activated K⁺ (12) and ATP-sensitive K⁺ channels (13). Comparatively, our previous study has demonstrated that rutaecarpine, a compound known to improve cerebral function, can block $I_{K(DR)}$ in a state-dependent manner in NG108-15 cells (14).

Voltage-gated K⁺ (K_v) channels play a major role in determining the excitability of neurons. These channels are responsible for setting the resting potential, repolarizing membranes during action potentials, regulating action potential duration and frequency (15). Among them, delayed rectifiers are ubiquitous in neurons. In fast-spiking neurons, a causal relationship between K_v3, especially K_v3.1, and the delayed rectifier K⁺ current ($I_{K(DR)}$), has now been well established (16). The K_v3 recombinant channel was reported to have properties suitable for the generation of high frequency firing. High activation threshold (~ -20 mV) and fast deactivation kinetics (<1 ms at resting potentials) of these K_v channels make them ideal for narrowing spike width and inter-spike interval. The $I_{K(DR)}$ containing K_v3 subunits has been known to contribute to changes in membrane potential in differentiated NG108-15 cells (14, 17).

The NG108-15 cell line has recently gained an interest by researchers as a suitable model for investigating the mechanisms of neuronal development and differentiation (18-20). It is a

hybrid cell line derived from the fusion of two separate cell lines, mouse neuroblastoma (N18TG-2, a subclone of mouse C1300 neuroblastoma cells) and rat glioma (C6BV-1, a subclone of rat C6 glioma) (18). Importantly, the K⁺ channels from the K_v3.1-K_v3.2 types, the activity of which mainly constitutes the generation of delayed rectifier K⁺ current ($I_{K(DR)}$) in NG108-15 cells, are responsible for spike repolarization and after-hyperpolarization of these cells (14, 18).

In this study, we intended to investigate the effect of LEV on ion currents in differentiated NG108-15 neuronal cells. Our experimental data and simulation results provide evidence that LEV can significantly suppress $I_{K(DR)}$, and this may constitute one of the underlying mechanisms through which LEV exert its anti-epileptic actions.

MATERIALS AND METHODS

Cell preparation and differentiation

The clonal strain NG108-15 cell line, formed by Sendai virus-induced fusion of the mouse neuroblastoma clone N18TG-2 and the rat glioma clone Cg BV-1, was originally obtained from the European Collection of Cell Cultures (ECACC-88112302; Wiltshire, UK). NG108-15 cells were kept in monolayer cultures at a density of 10⁶/cm² in plastic disks containing Dulbecco's modified Eagle's medium (Life Technologies; Grand Island, NY, USA) supplemented with 100 μM hypoxanthine, 1 μM aminopterin, 16 μM thymidine, and 5% fetal bovine serum as the culture medium, in a humidified incubator equilibrated with 90% air/10% CO₂ at 37°C (14). Media were replenished every 3 days with fresh media. The experiments were performed after 5 days of subcultivation.

To induce neuronal differentiation, culture medium was replaced with medium containing 1 mM dibutyryl cyclic-AMP and cells were cultured in the incubator for 1-7 days. NG108-15 cells could stop proliferating and show the growth of neurites in response to dibutyryl cyclic-AMP (20-21). The numbers of neurites and varicosities were found to be significantly increased in NG108-15 cells differentiated with dibutyryl cyclic AMP.

RNA isolation and reverse transcriptase-polymerase chain reaction (RT-PCR)

To detect the expression of K_v3.1 mRNA in NG108-15 cells treated with or without dibutyryl cyclic AMP, a semi-quantitative RT-PCR assay was carried out. Total RNA samples were extracted from NG108-15 cells with TRIzol reagent (Invitrogen, Grand Island, NY) and reverse-transcribed into complementary DNA using Superscript II reverse-transcriptase (Invitrogen, Grand Island, NY). The sequences of oligonucleotide primers used for K_v3.1 (NM_008421) were 5'-CGTGCCGACGAGTTCTTCT-3' and 5'-GGTCATCTCCAGCTCGTCCT-3' (22). Amplification of K_v3.1 was done using PCR SuperMix from Invitrogen under the following conditions: 35 cycles composed of 30 sec denaturation at 95°C, 30 sec primer annealing at 62°C, 1 min extension at 72°C, and followed by 72°C for the final extension for 2 min. PCR products were analyzed on 1.5% (w/v) agarose gel containing ethidium bromide and then visualized under ultraviolet light. Optical densities of DNA bands were scanned and quantified by AlphaImager 2200 (Alpha Innotech Corporation).

Isolation of cerebellar granule neurons

All animal experiments here were conducted in accordance with the specifications of the ethical committee of National

Cheng Kung University. Procedures for animal experimentation were reviewed and approved by the Institutional Animal Care and Use committee. Cerebellar granule cells were isolated from the Wistar rat pups of postnatal days 9-10. Cerebella of five to seven animals were excised after decapitation, and they were minced and digested with collagenase (50 mg/ml) for 10 min. Mechanical trituration was then performed by using a Pasteur pipette, in a DNAase I/soybean trypsin inhibitor solution (23). Dissociated cells were centrifuged and suspended in normal Tyrode's solution. Cells were used for experiments within 2-3 hours after isolation.

Electrophysiologic measurements

Cells were dissociated and an aliquot of cell suspension was transferred to a recording chamber mounted on the stage of an inverted DM-IL microscope (Leica Microsystems, Wetzlar, Germany) for experiment. The microscope was coupled to a digital video camera (DCR-TRV30; Sony, Tokyo, Japan) with a magnification up to 1500× to monitor cell size during the experiments. Cells were bathed at room temperature (20-25°C) in normal Tyrode's solution containing 1.8 mM CaCl₂. Patch pipettes were pulled from Kimax-51 glass capillaries (Kimble; Vineland, NJ, USA) on a PP-830 puller (Narishige, Tokyo, Japan) and fire-polished on an MF-83 microforge (Narishige). The resistances of the patch pipettes when filled with the internal solutions were between 3 and 5 MΩ. Ion currents were measured with glass pipettes in whole-cell configuration of the patch-clamp technique, using an RK-400 (Biologic, Claix, France) or an Axopatch 200B patch-clamp amplifier (Molecular Devices, Sunnyvale, CA, USA) (24). All potentials were corrected for liquid junction potential.

Data recordings and analyses

The signals were displayed on an analog/digital oscilloscope (HM-507; Hameg Inc., East Meadow, NY, USA) and on a Dell 2407WFP-HC color monitor (Round Rock, TX, USA). The data were stored online in a Slimnote VX₃ computer (Lemel, Taipei, Taiwan) via a universal serial bus port at 10 kHz through a Digidata-1322A interface (Molecular Devices), which was controlled by pCLAMP 9.0 software (Molecular Devices). Cell capacitance of 36-51 pF (47.3±6.3 pF; n=21) was compensated. Series resistance, in the range of 5-15 MΩ, was electronically compensated. The currents, low-pass filtered at 1 or 3 kHz, were stored and analyzed subsequently by use of pCLAMP 9.0 software (Molecular Devices), Origin 7.5 software (Microcal Software, Northampton, MA, USA), or custom-made macros built in Excel 2007 spreadsheet running on Windows Vista (Microsoft, Redmont, WA, USA). The pCLAMP-generated voltage-step protocols were used to measure the current-voltage (*I-V*) relations for ion currents. Action potential (AP) duration was measured at 90% of repolarization.

Concentration-response data for inhibition of $I_{K(DR)}$ were fitted with a modified form of the Hill equation:

$$y = \frac{(1-a) \times [\text{LEV}]^{-n_H}}{[\text{LEV}]^{-n_H} + \text{IC}_{50}^{-n_H}} + a,$$

where *y* is normalized amplitude of $I_{K(DR)}$; [LEV] represents the LEV concentration; and IC₅₀ and n_H are the concentration required for a 50% inhibition and Hill coefficient, respectively. Maximal inhibition (*i.e.*, 1-*a*) was also estimated.

Values were provided as means ±SEM with sample sizes (*n*) indicating the number of cells from which the data were taken. The paired or unpaired Student's *t*-test and one-way analysis of variance with the least-significance-difference method for

multiple comparisons were used for the statistical evaluation of differences among means. Statistical significance was determined at a P value of <0.05 .

Drugs and solutions

LEV (levetiracetam; (*S*)- α -ethyl-2-oxo-pyrrolidine acetamide; Keppra®) was kindly provided by UCB Pharma S.A. (Brussels, Belgium). Dibutyryl cyclic AMP, risperidone, tetraethylammonium chloride, and tetrodotoxin were purchased from Sigma Chemicals (St. Louis, MO, USA). The sea anemone toxin BDS-1, Apamin, margatoxin and iberiotoxin were obtained from Alomone Labs (Jerusalem, Israel). Nicorandil was kindly provided by Chugai Pharmaceutical (Tokyo, Japan). The double-distilled water that had been de-ionized through a Millipore-Q system (Bedford, MA, USA) was used in all experiments.

The composition of normal Tyrode's solution was 136.5 mM NaCl, 5.4 mM KCl, 1.8 mM CaCl₂, 0.53 mM MgCl₂, 5.5 mM glucose, and 5.5 mM HEPES-NaOH buffer, pH 7.4. To record K⁺ currents or membrane potential, the patch pipette was filled with a solution consisting of 140 mM KCl, 1 mM MgCl₂, 3 mM Na₂ATP, 0.1 mM Na₂GTP, 0.1 mM EGTA, and 5 mM HEPES-KOH buffer, pH 7.2. To record $I_{K(\text{erg})}$, high-K⁺, Ca²⁺-free solution contained a solution consisting of 130 mM KCl, 10 mM NaCl, 3 mM MgCl₂, 6 mM glucose, and 10 mM HEPES-KOH buffer, pH 7.4. To measure Na⁺ or Ca²⁺ currents, K⁺ ions inside the pipette solution were replaced with equimolar Cs⁺ ions, and the pH was adjusted to 7.2 with CsOH.

Computer simulations

To simulate neuronal firing in this study, a theoretical model which consists of the fast inward Na⁺ current (I_{Na}), the classical HH-type K⁺ current (I_{K}), and the delayed rectifier K⁺ current (I_{Kdr}) was mathematically constructed to mimic neuronal firing in differentiated NG108-15 cells (Table 1). The modeled cell behaves according to the modified Hodgkin-Huxley (HH) scheme. The equation for V is given by:

$$C_m \frac{dV}{dt} = -I_{\text{Na}} + I_{\text{K}} + I_{\text{K(DR)}} + I_{\text{L}} + I_{\text{app}} + I_{\text{noise}},$$

where t is the time (msec); V is membrane potential (mV); C_m is the membrane capacitance ($\mu\text{F}/\text{cm}^2$); I_{Na} is Na⁺ current; I_{K} is the classical HH-type K⁺ current; I_{Kdr} is K_v3.1-encoded current; I_{L} is a leak current; I_{app} is the injected current ($\mu\text{A}/\text{cm}^2$); and I_{noise} represents the effect of unbiased white noise.

The rate constants used in the simulation were, for I_{Na} :

$$\begin{aligned} \alpha_m &= 0.1 \times (V + 40) / \{1 - \exp[-0.1 \times (V + 40)]\}, \\ \beta_m &= 4 \times \exp[-0.055 \times (V + 65)], \\ \alpha_h &= 0.07 \times \exp[-0.05 \times (V + 70)], \\ \beta_h &= 1 / \{1 + \exp[-0.1 \times (V + 35)]\}, \end{aligned}$$

for the classical HH-type I_{K} :

$$\begin{aligned} \alpha_n &= 0.01 \times (V + 55) / \{1 - \exp[-0.1 \times (V + 55)]\}, \\ \beta_n &= 0.125 \times \exp[-0.0125 \times (V + 65)], \end{aligned}$$

and, for K_v3.1-encoded $I_{\text{K(DR)}}$:

$$\begin{aligned} \alpha_{n3} &= -0.021 \times (V + 8.3 + \eta) / \{\exp(-(V + 8.3 + \eta)/9.8) - 1\}, \\ \beta_{n3} &= 0.0002 \times \exp(-(V + 23.6 + \eta)/20.7), \\ \gamma_{n3} &= 1 / (\alpha_{n3} + \beta_{n3}), \end{aligned}$$

where τ_{n3} is the activation time constant of K_v3 current., and η is the value used to mimic effect of LEV in which the shift of

voltage-dependent activation was altered. Because the slowly inactivating I_{Kdr} in NG108-15 cells is a state-dependent process, the form of the equation describing the inactivation variables was modified as follows (25, 26):

$$dh_{K3}/dt = 0.0005 \times (1 - h_{K3}) - 0.0014 \times n_3 \times h_{K3},$$

The current I_{noise} , which represents the effect of channel noise, is given by:

$$I_{\text{noise}} = \sigma_N \times \omega,$$

where σ_N is the noise amplitude and ω is a Wiener variable.

Simulations were undertaken in C++ programming language or within the simulation package XPPAUT on a Hewlett Packard Workstation (HPxw9300; Palo Alto, CA) (27, 28). Source files used in this study can be available from <http://senselab.med.yale.edu/senselab/modeldb> or at a supplementary file in this article. The information for XPP software is readily available at <http://www.math.pitt.edu/~bard/XPP/XPP.html>. Several different integration algorithms (*e.g.*, backwards Euler and Cvode) and time steps were used to check accuracy and stability.

A simulated network of spiking neurons with Hodgkin-Huxley type (21, 29) was also undertaken to reflect the conditions in which LEV was applied. This model consists of two populations of excitatory (100 cells) and inhibitory (50 cells) neurons with random connectivity, in which Hodgkin-Huxley kinetics was generated. The slowly inactivating $I_{\text{K(DR)}}$, which resembles the properties of $I_{\text{K(DR)}}$ seen in differentiated NG108-15 cells, was also incorporated to the model. As current injections were randomly applied to the neurons, persistent and stochastic activity of neuronal spiking can be readily simulated. Within the network, neurons can also communicate *via* a simplified synaptic connection.

RESULTS

The mRNA expression for $K_v3.1$ in differentiated NG108-15 cells

In NG108-15 cells, as the $I_{\text{K(DR)}}$ was to be carried by the Shaw-related K⁺ channels, the product of $K_v3.1$ (or KCNC1) gene, we examined the mRNA levels of $K_v3.1$ on NG108-15 cells cultured in conditions promoting cell differentiation. Cells were differentiated after being cultured with 1 mM dibutyryl cyclic AMP for 7 days. Our RT-PCR analysis demonstrated that the mRNA of $K_v3.1$ subunit in cells treated with dibutyryl cyclic AMP was detected. In addition, in our experimental conditions, the extent of mRNA expression for $K_v3.1$ in differentiated cells was found to be significantly increased (Fig. 1).

Table 1. Default parameters used for the implementation of a modeled neuron in this study.

Symbol	Description	Value
C_m	Membrane capacitance	1.0 $\mu\text{F}/\text{cm}^2$
G_{Na}	Na ⁺ current conductance	40 mS/cm ²
G_{K}	Classic HH-type K ⁺ current conductance	2.0 mS/cm ²
G_{Kdr}	Delayed-rectifier K ⁺ current conductance	1.0 mS/cm ²
G_{leak}	Leak current conductance	0.03 mS/cm ²
V_{Na}	Na ⁺ reversal potential	+50 mV
V_{K}	K ⁺ reversal potential	-80 mV
V_{L}	Reversal potential for leak current	-49 mV

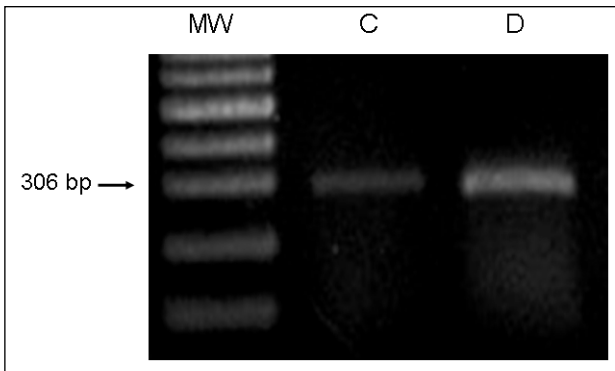


Fig. 1. The expression levels of the $K_v3.1$ mRNA isolated from normal (C) and differentiated (D) NG108-15 cells. Total RNA was isolated and RT-PCR analysis was performed. Amplified RT-PCR products were obtained using for a marker lane of DNA molecular size (leftmost lane; MW) and $K_v3.1$ subunit (306 bp). The PCR replicates were 35 cycles and the fold difference in the density of the bands is almost 3 fold (74.6%/25.4%). Notably, cell differentiation with dibutyryl cyclic AMP (1 mM) increases the mRNA level of $K_v3.1$ subunit as compared with that in normal cells.

Effect of LEV on delayed rectifier K^+ current ($I_{K(DR)}$)($K_v3.1$) in differentiated NG108-15 cells

In an initial set of experiments, the whole-cell configuration of the patch-clamp technique was used to evaluate the effect of LEV on ion currents in differentiated NG108-15 cells. To record K^+ outward currents, cells were bathed in Ca^{2+} -free Tyrode's solution which contained tetrodotoxin (1 μ M) and $CdCl_2$ (0.5 mM). When the cell was held at -50 mV, depolarizing voltage pulses from -50 to different voltages in 10 mV increments were applied with a duration of 300 msec, a family of large K^+ outward currents with little inactivation was elicited (Fig. 2). These outward currents have been identified as $I_{K(DR)}$ (14, 17). When cells were exposed to LEV (30 μ M), the amplitude of $I_{K(DR)}$ measured at the end of the voltage pulses was reduced at the potentials ranging from 0 to $+50$ mV. For example, when depolarizing pulses from -50 to $+30$ mV were applied, LEV (30 μ M) significantly decreased current amplitude at the end of the voltage pulses from 1685 ± 198 to 945 ± 44 pA ($n=8$, $P<0.05$). After washout, the amplitude of $I_{K(DR)}$ at $+30$ mV was partially returned to 1632 ± 102 pA ($n=6$). However, when

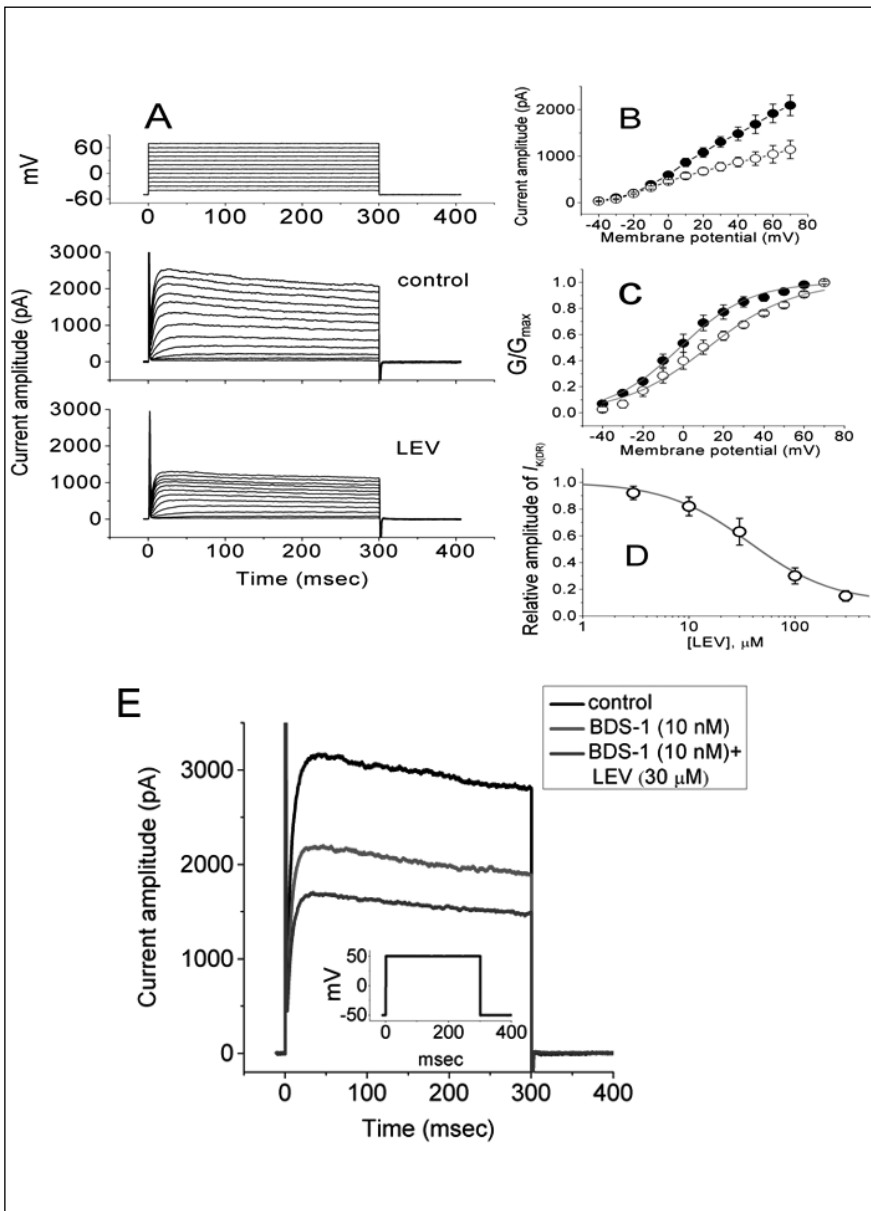


Fig. 2. Inhibition of LEV on delayed rectifier K^+ current ($I_{K(DR)}$) in NG108-15 cells differentiated with 1 mM dibutyryl cAMP. In these experiments, cells were bathed in Ca^{2+} -free Tyrode's solution containing 0.5 mM $CdCl_2$. Pipette was filled with a K^+ -containing solution. (A) Original current traces obtained in the absence (upper) and presence (lower) of 30 μ M LEV. The uppermost part shown in A indicates the voltage protocol used. (B) The I - V relationships of $I_{K(DR)}$ under control and during the exposure to LEV (30 μ M). ●: control; ○: LEV. (C) Comparison of conductance-voltage relationships of $I_{K(DR)}$ between the absence (●) and presence (○) of LEV. The smooth lines were well fit to a Boltzmann function as described in Materials and Methods. Notably, LEV could shift the activation curve of $I_{K(DR)}$ to more depolarized potential by approximately 10 mV. (D) Concentration-response relationship for LEV-induced inhibition of $I_{K(DR)}$. Each point represents the mean \pm SEM ($n=5-8$). The gray smooth line represents the best fit to the Hill equation as described in Materials and Methods. The IC_{50} value, maximally inhibited percentage of $I_{K(DR)}$ and Hill coefficient were 37 μ M, 100% (*i.e.*, $\alpha=0.1$), and 1.1, respectively. (E) Effect of BDS-1 on delayed rectifier K^+ current ($I_{K(DR)}$) in differentiated NG108-15 cells. Cells were bathed in Ca^{2+} -free solution containing 1 μ M tetrodotoxin. Black trace is control, red trace was obtained after application of BDS-1 (10 nM) and blue trace was recorded after addition of LEV (30 μ M), but in continued presence of BDS-1. The inset indicates the voltage protocol used.

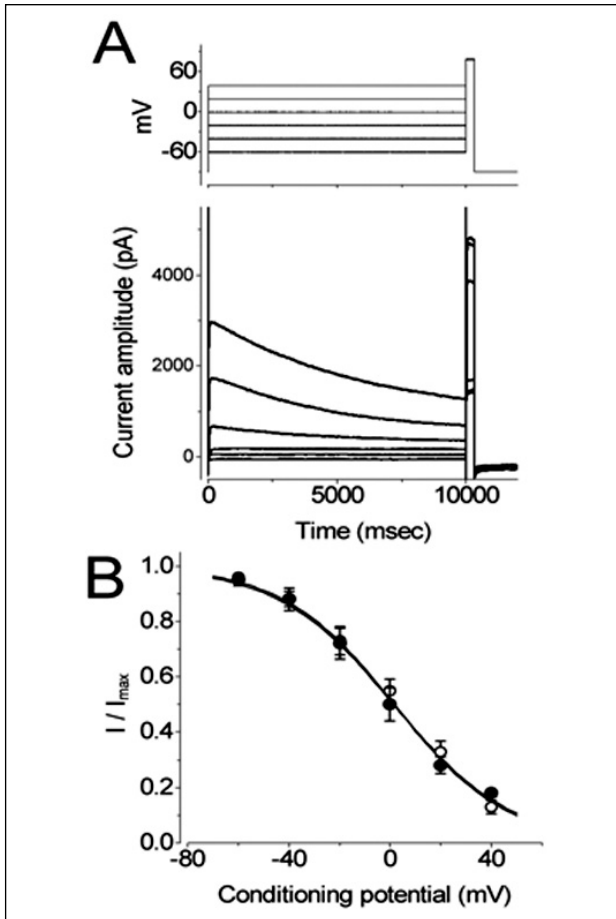


Fig. 3. Steady-state inactivation of $I_{K(DR)}$ in the absence and presence of LEV in differentiated NG108-15 cells. With aid of a double-pulse protocol, the steady-state inactivation parameters of $I_{K(DR)}$ were determined. (A) Superimposed current traces obtained in the control condition. Similar to that in Fig. 2, the uppermost part shown in A indicates the voltage protocol used. (B) Normalized amplitude of $I_{K(DR)}$ (I/I_{max}) was constructed against the conditioning potential, and the smooth curves were well fitted by the Boltzmann equation. Each point represents the mean \pm SEM ($n=5-8$). \bullet : control; \circ : LEV (30 μ M). There is no change in steady-state inactivation curve of $I_{K(DR)}$ during exposure to LEV.

the pipettes were filled with a solution containing 100 μ M LEV, no detectable change in the amplitude of $I_{K(DR)}$ was observed.

The effect of LEV on the conductance-voltage relationship of $I_{K(DR)}$ in NG108-15 cells was also evaluated and the experimental data are shown in Fig. 2C. In Fig. 2C, the normalized conductance of $I_{K(DR)}$ (*i.e.*, G/G_{max}) was constructed against the membrane potential and the curves were fitted by a Boltzmann function using least-squares method:

$$G = \frac{G_{max}}{1 + \exp[-(V - a)/b]},$$

where G_{max} is the maximal conductance of $I_{K(DR)}$, V is the membrane potential in mV, a is the membrane potential for half-maximal activation, and b is the slope factor of the inactivation curve. In the absence of LEV, $a = -1.7 \pm 0.9$ mV and $b = 17.1 \pm 1.1$ mV ($n=5$), whereas in the presence of LEV (30 μ M), $a = 12.2 \pm 1.2$ mV, $b = 19.7 \pm 1.4$ mV ($n=5$). LEV (30 μ M) could thus shift the midpoint of the activation curve toward depolarizing voltage by approximately 10 mV, although no significant change

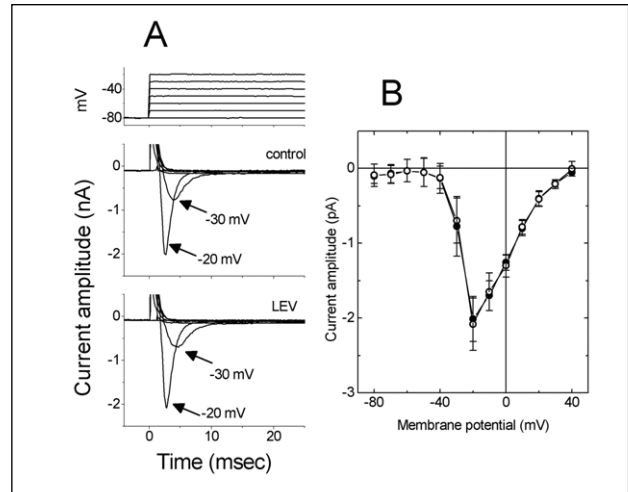


Fig. 4. No effect of LEV on I_{Na} in differentiated NG108-15 cells. In these experiments, cells were bathed in Ca^{2+} -free Tyrode's solution containing 0.5 mM $CdCl_2$ and 10 mM tetraethylammonium chloride. Pipette was filled with a Cs^+ -containing solution. A, Original current traces obtained in the absence (upper) and presence (lower) of 30 μ M LEV. The arrow indicates the level of depolarizing pulse applied. B, $I-V$ relationships of I_{Na} under control and during the exposure to LEV (30 μ M). Each point represents the mean \pm SEM ($n=5-8$). \bullet : control; \circ : LEV (30 μ M).

in the slope factor (*i.e.*, b) was detected in the presence of LEV. Thus, there was a positive shift voltage-dependence of the steady-state activation curve of $I_{K(DR)}$ in the presence of LEV.

The relationship between the LEV concentration and the percentage inhibition of $I_{K(DR)}$ was also constructed in this study. In these experiments, each cell was depolarized from -50 to +50 mV with a duration of 300 msec. Current amplitudes were measured at the end of depolarizing pulses. As shown in Fig. 2D, LEV (1 μ M – 1 mM) suppressed the amplitude of $I_{K(DR)}$ in a concentration-dependent manner. The IC_{50} value for LEV-induced inhibition of $I_{K(DR)}$ was 37 μ M. This drug at a concentration of 300 μ M almost completely suppressed the amplitude of $I_{K(DR)}$. The results demonstrate that LEV has a significant depressant action on $I_{K(DR)}$ functionally expressed in differentiated NG108-15 cells.

To further clarify if the LEV's sensitive component of $I_{K(DR)}$ is mediated by Kv3.1, we applied the sea anemone toxin BDS-1, which is reported to be an effective inhibitor of Kv3.1 (30). As shown in Fig. 2E, BDS-1 at a concentration of 10 nM is effective in suppressing the amplitude of $I_{K(DR)}$. Subsequent application of LEV can further decrease the amplitude of $I_{K(DR)}$. The additive effects of BDS-1 and LEV suggest the binding sites of BDS-1 and LEV on the K_V channel in NG108-15 cells might be different. This results demonstrate LEV-sensitive component of $I_{K(DR)}$ is mediated by Kv3.1.

Effect of LEV on steady-state inactivation of $I_{K(DR)}$

The effect of LEV on the steady-state inactivation of $I_{K(DR)}$ in differentiated NG108-15 cells was also evaluated. In this series of experiments, cells were bathed in Ca^{2+} -free Tyrode's solution and the steady-state inactivation parameters of $I_{K(DR)}$ were determined with or without application of LEV (30 μ M) under the aid of double-pulse protocol (Fig. 3). In Fig. 3B, the normalized amplitude of $I_{K(DR)}$ (*i.e.*, I/I_{max}) was constructed against the conditioning potential and the curves were fitted by

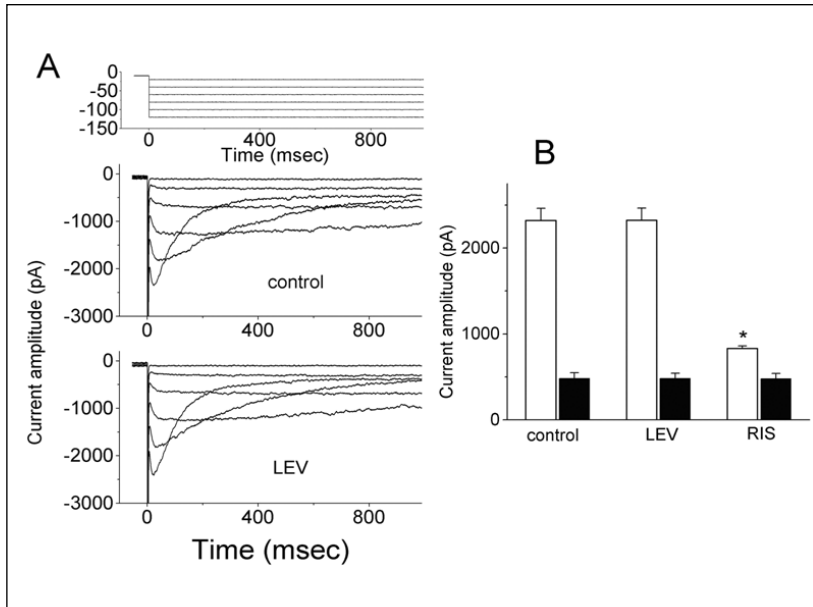


Fig. 5. Lack of effect of LEV on $I_{K(erg)}$ in differentiated NG108-15 cells. In these experiments, cells, bathed in a high- K^+ , Ca^{2+} -free solution, were held at -10 mV, and various potentials from -20 to -120 mV with 20 -mV decrements was applied at a rate of 0.05 Hz. In (A) superimposed current traces shown in the upper part are control, and those in the lower part were result obtained 2 min after application of LEV ($30 \mu M$). The voltage protocol used is illustrated in the uppermost part. In (B) summary of the data shows the effect of LEV and risperidone on $I_{K(erg)}$. Current amplitude at the level of -120 mV was obtained at the beginning (open box) and end (filled box) of hyperpolarization pulse. LEV: $30 \mu M$ LEV; RIS: $3 \mu M$ risperidone. Each bar indicates the mean \pm SEM ($n=5-6$). *Significantly different from control. Notably, LEV had no effect on the peak amplitude of $I_{K(erg)}$, while risperidone was effective in suppressing it.

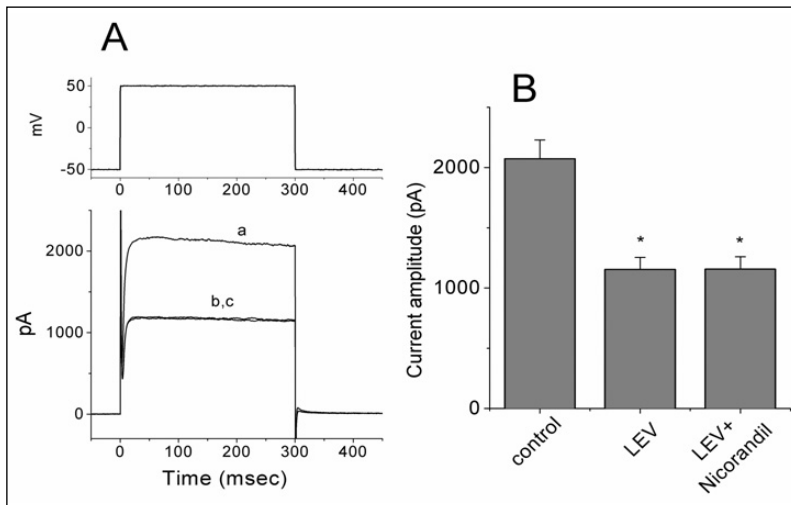


Fig. 6. Lack of effect of LEV on $I_{K(ATP)}$ in differentiated NG108-15 cells. In these experiments, cells were bathed in Ca^{2+} -free Tyrode's solution containing 0.5 mM $CdCl_2$. Pipette was filled with a K^+ -containing solution. The current tracings in panel A show control (a), LEV ($30 \mu M$) (b), and LEV ($30 \mu M$) plus nicorandil ($30 \mu M$). Panel B is the summary of data showing effects of LEV and LEV plus nicorandil on the amplitude of $I_{K(DR)}$ in NG 108-15 cells. Notably, lack of nicorandil effect on LEV-induced inhibition of $I_{K(DR)}$ was observed.

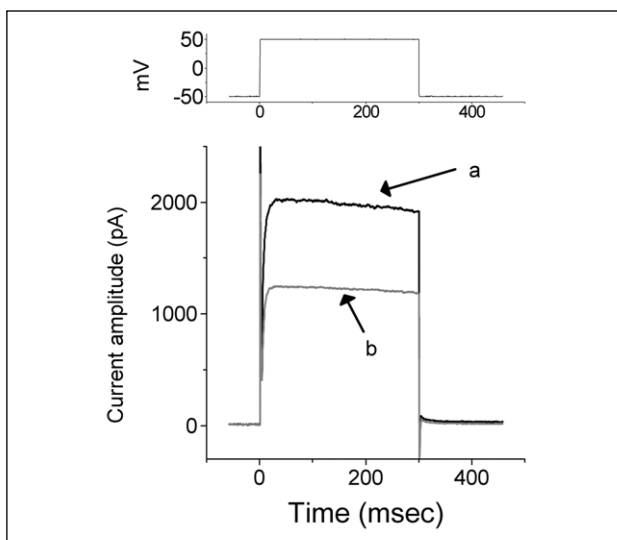


Fig. 7. Inhibitory effect of LEV on $I_{K(DR)}$ in isolated cerebellar granule cells. $I_{K(DR)}$ was elicited by depolarizing pulse from -50 to $+50$ mV with a duration of 300 msec. The current tracings show control (a) and LEV (b). The upper part indicates the voltage protocol used.

a Boltzmann function similar to those used for the activation curve of $I_{K(DR)}$ presented above. The results showed that although a significance decrease in maximal conductance of $I_{K(DR)}$ was found, neither the midpoint of inactivation curve nor the slope factor was altered in the presence of $30 \mu M$ LEV (Fig. 3).

Effect of LEV on voltage-dependent Na^+ current (I_{Na}) in differentiated NG108-15 cells

Brivaracetam, a novel high-affinity SV2A ligand and a chemically related LEV, has been recently recognized to exert effects on I_{Na} (31). Moreover, there was an increase in the expression levels of $Na_v1.7$ in NG108-15 cells when neuronal differentiation was induced by pretreatment with a cyclic AMP analogue (20, 21). The effects of LEV on I_{Na} were thus investigated in these cells. The experiments were conducted with a Cs^+ -containing pipette solution. Each cell was held at the level of -80 mV and different depolarizing pulses (25 msec in duration) were delivered at a rate of 0.1 Hz. As shown in Fig. 4, LEV ($30 \mu M$) was found to have no effects on the peak amplitude of I_{Na} . For example, when the cell was depolarized from -80 to -20 mV, application of LEV ($10 \mu M$) did not affect the peak amplitude of I_{Na} (2.0 ± 0.3 versus 2.1 ± 0.4 nA; $n=6$,

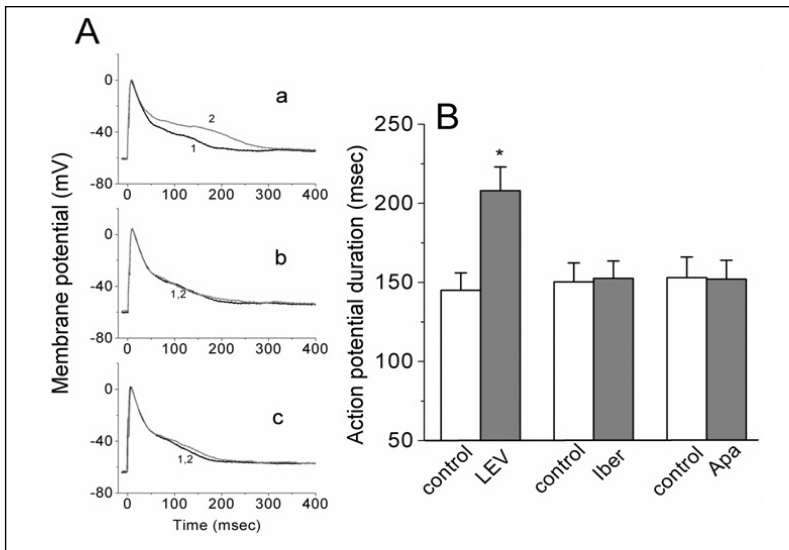


Fig. 8. Effect of LEV on action potentials (APs) in differentiated NG108-15 cells. Cells were bathed in normal Tyrode's solution containing 1.8 mM CaCl_2 . Current-clamp configuration was made and pipettes were filled with a K^+ -containing solution. (A) Original potential traces obtained in the absence and presence of 30 μM LEV (a), 200 nM iberiotoxin (b), or 200 nM apamin (c). (B) Summary of the data showing the effects of LEV, iberiotoxin, and apamin on AP duration in NG108-15 cells. Each point represents the mean \pm SEM ($n=6-8$). Notably, unlike iberiotoxin or apamin, LEV can significantly increase AP duration. 1 and 2 means before and after addition of drugs.

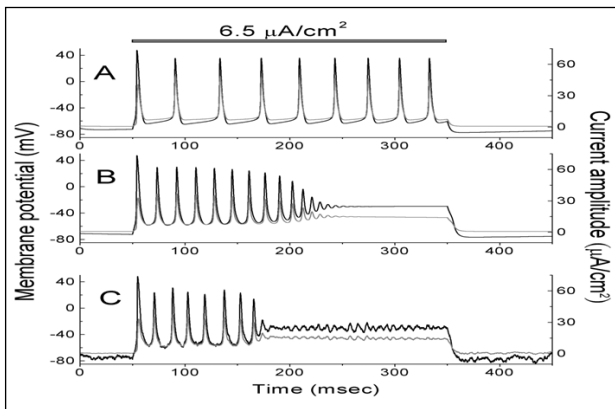


Fig. 9. Simulation modeling used to mimic LEV effects on the firing of APs in a modeled neuron. The model as described in Materials and Methods was developed based on the HH scheme in which the $I_{\text{K(DR)}}$ (*i.e.*, $\text{K}_{\text{v}3.1}$ -encoded K^+ current) was included. In A, simulated firing of APs was elicited in response to a 300-msec current stimulus (6.5 $\mu\text{A}/\text{cm}^2$) as indicated by horizontal bar. In B, when the $I_{\text{K(DR)}}$ conductance ($G_{\text{K(DR)}}$) was arbitrarily decreased from 1.0 to 0.7 mS/cm^2 , along with shift of steady-state activation curve of $I_{\text{K(DR)}}$ to more depolarized voltage by +10 mV, the amplitude of $I_{\text{K(DR)}}$ was readily reduced, together with termination in the firing of neuronal APs. In C, when the noisy fluctuation of current amplitude was incorporated to the modeled neuron, the termination of APs in response to membrane depolarization was further facilitated. Notably, black lines represent simulated potential tracings, whereas gray lines indicate the time course of simulated $I_{\text{K(DR)}}$.

$P > 0.05$). Moreover, no change in the I - V relationship of I_{Na} was observed in the presence of 30 μM LEV (Fig. 4B). Thus, experimental results indicate that unlike brivaracetam, LEV has little or no effect on I_{Na} in these cells.

Effect of LEV on erg-mediated K^+ current ($I_{\text{K(erg)}}$) in differentiated NG108-15 cells

We further investigated whether LEV affects the amplitude of $I_{\text{K(erg)}}$ present in differentiated NG108-15 cells. In these experiments, cells were bathed in a high K^+ , Ca^{2+} -free solution. A family of large inward deactivating currents in response to

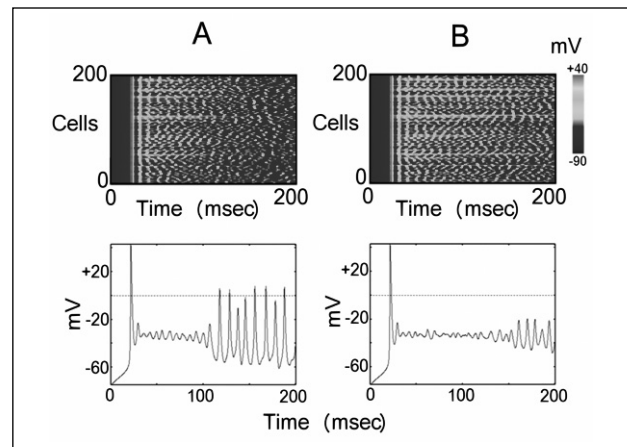


Fig. 10. Array plots of a modified HH type neuronal network used to mimic effects of LEV. A: control. B: $I_{\text{K(DR)}}$ conductance was reduced from 7 to 4 mS/cm^2 and the activation curve of $I_{\text{K(DR)}}$ was shifted by +10 mV. The traces shown below indicate the firing of APs present in 4th excitatory modeled neuron. Notably, a decrease in I_{Na} conductance causes a reduction of the firing, along with increased irregularity of neuronal firing. The combination of decreased conductance of $I_{\text{K(DR)}}$ and depolarized shift of voltage-dependent activation of $I_{\text{K(DR)}}$, in which the effect of LEV is mimicked, can terminate the firing in simulated network of neurons in a stochastic fashion.

membrane hyperpolarizations (*i.e.*, $I_{\text{K(erg)}}$) could be observed in these cells (32). As shown in Fig. 5, when the cell was hyperpolarized from -10 to different voltages with a duration of 1 sec, cell exposure to LEV (30 μM) was found to have no significant effect on the amplitude of deactivating $I_{\text{K(erg)}}$ seen in differentiated NG108-15 cells. However, risperidone at a concentration of 3 μM can suppress deactivating $I_{\text{K(erg)}}$ effectively. Therefore, $I_{\text{K(erg)}}$ present in these cells is apparently not subject to inhibition by LEV.

Effect of LEV on ATP-sensitive K^+ current ($I_{\text{K(ATP)}}$) in differentiated NG108-15 cells

For further delineation of the ionic effect of LEV, we then investigated if LEV exerts effects on $I_{\text{K(ATP)}}$ present in differentiated

NG108-15 cells. Cells were bathed in Ca^{2+} -free Tyrode's solution containing 0.5 mM CdCl_2 and the recording pipettes were filled with a K^+ -containing solution. As shown in Fig. 6, when depolarizing pulses from -50 to $+50$ mV were applied, LEV (30 μM) significantly decreased current amplitude at the end of the voltage pulses from 2012 ± 198 to 1101 ± 44 pA ($n=8$, $P < 0.05$, Fig. 6A). However, when nicorandil (30 μM), an $I_{\text{K(ATP)}}$ agonist, was further applied, its inability to reverse LEV-induced decrease of $I_{\text{K(DR)}}$ was demonstrated. Fig. 6B depicts the summarized data showing the effects of LEV and LEV plus nicorandil on the amplitude of $I_{\text{K(DR)}}$ in NG 108-15 cells. In addition, nicorandil (30 μM) alone had no effect on $I_{\text{K(DR)}}$ and a subsequent application of LEV (30 μM) reduced the amplitude of $I_{\text{K(DR)}}$. This lack of nicorandil effect shown here suggests that LEV-induced inhibition of $I_{\text{K(DR)}}$ was not mediated by inhibition of $I_{\text{K(ATP)}}$.

Effect of LEV on $I_{\text{K(DR)}}$ in cerebellar granular cells

Previous studies have demonstrated that one of the adverse effects for LEV is giddiness. As cerebellum is one of the preferential binding sites for LEV and whether the giddiness might be related to effect of LEV on $I_{\text{K(DR)}}$ in cerebellum is unknown. Therefore, we further investigated the effect of LEV on isolated cerebellar granular cells. In isolated cerebellar granule cells, $I_{\text{K(DR)}}$, which was identified as a slowly inactivating $I_{\text{K(DR)}}$, could be elicited. As shown in Fig 7, LEV was effective in suppressing the amplitude of $I_{\text{K(DR)}}$ present in these cells. When depolarizing pulses from -50 to $+50$ mV were applied, LEV (30 μM) significantly decreased current amplitude at the end of the voltage pulses from 2018 ± 152 to 1196 ± 81 pA ($P < 0.05$). Similar results were obtained in other seven different cells.

Effect of LEV on Action Potentials (APs) in differentiated NG108-15 cells

In another series of experiments, we examined the effect of LEV on changes in membrane potential. In these experiments, differentiated NG 108-15 cells were bathed in normal Tyrode's solution which contained 1.8 mM CaCl_2 . Current-clamp recordings were made with a K^+ -containing pipette solution. The typical effect of LEV on APs in NG108-15 cells is illustrated in Fig. 8. LEV at a concentration of 30 μM significantly prolonged the AP duration to 208 ± 15 msec from a control value of 148 ± 11 msec ($n=8$). However, neither iberiotoxin (200 nM) nor apamin (200 nM) was found to have any effects on the duration of APs in these cells (Fig. 8B). Iberiotoxin and apamin are known blockers of large- and small-conductance Ca^{2+} -activated K^+ channels, respectively. The effect of LEV on spike broadening in NG108-15 cells could be due mainly to its inhibitory action on $I_{\text{K(DR)}}$, but not on Ca^{2+} -activated K^+ currents.

Simulation modeling mimicking LEV effects on the firing of APs in a modeled neuron

The model as described in MATERIALS AND METHODS was developed based on the Hodgkin-Huxley scheme in which the $I_{\text{K(DR)}}$ (i.e., $\text{K}_v3.1$ -encoded K^+ current) was included. Simulated firing of APs was elicited in response to a 300-msec current stimulus (6.5 $\mu\text{A}/\text{cm}^2$) as indicated by horizontal bar (Fig. 9A). When the $I_{\text{K(DR)}}$ conductance ($G_{\text{K(DR)}}$) was decreased from 1.0 to 0.7 mS/cm^2 , along with a more positive shift of steady-state activation curve of $I_{\text{K(DR)}}$ by +10 mV, the amplitude of $I_{\text{K(DR)}}$ was reduced and the firing of neuronal APs eventually terminated (Fig. 9B). In addition, when the noisy fluctuation of current amplitude was incorporated to the modeled neuron, the termination of APs in response to membrane depolarization was accentuated (Fig. 9C).

Modified Hodgkin-Huxley type neuronal network mimicking effects of LEV

A decrease in I_{Na} conductance causes a reduction of the firing, along with increased irregularity of neuronal firing (Fig. 10A). When $I_{\text{K(DR)}}$ conductance was reduced from 7 to 4 mS/cm^2 and the activation curve of $I_{\text{K(DR)}}$ was shifted by +10 mV, in which the LEV effect is mimicked, the firing in simulated network of neurons terminated (Fig. 10B).

DISCUSSION

The major findings of this study are as follows. First, in differentiated NG108-15 neuronal cells, LEV inhibited the amplitude of $I_{\text{K(DR)}}$ in a concentration-dependent manner. Second, LEV could produce a depolarized shift in the steady-state activation curve of $I_{\text{K(DR)}}$. Third, neither I_{Na} nor $I_{\text{K(erg)}}$ was affected after application of LEV. Fourth, LEV could prolong the duration of APs in these cells. Fifth, the simulation model predicted that the decreased conductance of $I_{\text{K(DR)}}$ with a depolarized shift in activation curve of $I_{\text{K(DR)}}$, which reflected the LEV action, could terminate the firing of APs in modeled neurons and in a simulated network of neurons with HH kinetics. Taken together, the inhibition by LEV of $I_{\text{K(DR)}}$ can be one of the ion mechanisms underlying LEV-induced change in functional activity of neurons.

Consistent with previous studies (14, 18), NG108-15 cell line was found to express $\text{K}_v3.1$ mRNAs and to exhibit the activity of the slowly inactivating delayed rectifier K^+ channels. An important characteristic for the majority of $I_{\text{K(DR)}}$ in differentiated NG108-15 cells is that it activates rapidly and inactivates slowly. The activation time constant ranges from 5 to 15 msec at the potentials between +30 and +70 mV. It inactivates slowly from several hundreds to several thousands of milliseconds during sustained depolarization. The kinetics of $\text{K}_v3.1$ -encoded current thus fit well with these properties (16). In addition to fast-spiking interneurons, K_v3 channels are present in many central neurons including hippocampal pyramidal neurons (33) and Purkinje cells (34). In the light of the present results and previous studies, it seems that $\text{K}_v3.1$ currents are likely to be the major molecular component of $I_{\text{K(DR)}}$ in NG108-15 cells. Inability of margatoxin (100 nM) or agitoxin-2 (100 nM) to produce any effects on $I_{\text{K(DR)}}$ in NG108-15 cells (data not shown) suggests a lack of functional expression of K_v1 subunits in NG108-15 cells. However, given that the kinetics of $\text{K}_v3.1$ currents expressed in heterologous systems can be regulated by interaction with auxiliary subunits, small Ca^{2+} -binding proteins and phospholipids (35), it seems not possible to use biophysical properties alone to identify the molecular correlate of a given K_v current. Nevertheless, this cell line can be a useful model with which to study the biophysical and pharmacological properties of $\text{K}_v3.1$ channel.

Previous reports showed that piracetam, another structurally related compound of LEV, was found to suppress the amplitude of Ca^{2+} -activated K^+ currents in neurons (11). However, neither apamin nor iberiotoxin had any effects on the duration of APs in differentiated NG108-15 cells. Thus it is unlikely that small- or large-conductance Ca^{2+} -activated K^+ currents are responsible for LEV-induced reduction of K^+ currents in NG108-15 cells. Similarly, LEV-induced inhibition of $I_{\text{K(DR)}}$ could not be reversed by further application of nicorandil (30 μM). LEV-induced block of $I_{\text{K(DR)}}$ presented here is also unlinked to inhibition of ATP-sensitive K^+ channels (13, 28).

Intracellular dialysis with LEV was found to have no effect on $I_{\text{K(DR)}}$ in NG108-15 cells. The results suggest that the LEV binding site is closer to the extracellular rather than the

intracellular face of the cell membrane. Importantly, the IC_{50} value of LEV required for the inhibition of $I_{K(DR)}$ in these cells was $37 \mu\text{M}$. It is thus clear that the concentration of LEV used to suppress $I_{K(DR)}$ is compatible to clinically relevant concentrations (36). In addition to the anti-epileptic effect, the giddiness in LEV therapy might be related, at least partially, to the effect of LEV on $I_{K(DR)}$ in cerebellum. As cerebellar granule cells send excitatory parallel fibers up through the Purkinje layer into the molecular layer. Additionally, it remains to be determined to what extent LEV-induced inhibition of $I_{K(DR)}$ shown here contributes to psychotic reaction caused by this drug as describe previously (37).

The fast delayed rectifier current (K_v3) activated much slower than the classical delayed rectifier found in the squid giant axons. Notably, in the paper by Madeja, *et al.* (9), the simulation results were derived from the classical HH type K^+ current which is low-threshold and near to the level of resting potential. However, in our study, high-threshold $I_{K(DR)}$, which is relatively insensitive to the level of resting potential, was incorporated to the modified model. Because of different kinetics of these two K^+ currents (38), their effects on the firing of neuronal action potentials are different. In addition, due to the steep voltage dependence of current amplitude and the high activation threshold, these fast delayed rectifier currents do repolarize action potentials but little contribute to the resting membrane potential (38). In K_v3 expressing neurons, with a narrowing spike width and inter-spike interval, this shortened spike width in turn reduces inactivation of Na^+ channels and leads to fast-spiking activity (38, 39). In more fast-spiking epileptic neurons in cerebral cortex or hippocampus, the inhibitory effect on K_v3 , especially $K_v3.1$, would provide a more potential anti-epileptic role, as compared with the effects on normal firing neurons. Notably, a partial block of the classical HH K^+ current leads to the increased number of evoked APs, whereas a partial block of the slow delayed rectifier current (*e.g.*, $K_v3.1$ -encoded current) decreases the number of evoked APs (40). Interestingly, in a prior study on $K_v3.1$ channel-deficient mice ($K_v3.1^{-/-}$), contrary to expectation, homozygous $K_v3.1^{-/-}$ mice do not have increased spontaneous seizure activity (41).

Additionally, LEV has been approved as an effective treatment in generalized epilepsy (4). Animal studies of generalized epilepsy have provided strong evidence for pathological involvement of thalamic reticular neurons (42); as $K_v3.1$ K^+ channels are substantially expressed in thalamic reticular neurons (43) and inhibition of these channels had been shown to display action potential broadening and reduced fast afterhyperpolarization (44). It is anticipated that LEV could have effects on thalamocortical function, although further investigation is needed.

The SV2A, a presynaptic vesicle protein, was thought to be involved in synaptic vesicle exocytosis and neurotransmitter release (45). Several studies have demonstrated that the synaptic vesicle protein 2A (SV2A), a presynaptic vesicle protein, is the binding site of LEV in the brain, with which this drug can interact to modulate the function of SV2A (1, 6, 46, 47). With the aid of the LAIGN program, we further evaluated the similarity of amino-acid sequence between the SV2A protein and the α -subunit of $K_v3.1$. Notably, the portion in $K_v3.1$ α -subunit (human: NP_001106212), to which the sequence of SV2A (human: AAH00776) shares the similarity (36.2% identity), was found to be located extracellularly at 385-431. This region was located in the S6 segment of the $K_v3.1$ channel. This comparison leads us to speculate that the LEV molecule binds to similar docking region(s) to block $I_{K(DR)}$ as well as to interact with SV2A protein.

In fact, cortical neurons *in vivo* are subject to varying overall levels of stochastic synaptic background activity, which is particularly intense during active states of the brain (48). The

noise itself is shown to generate an effective potential function for the dynamics that is asymmetric and bistable. In our simulations, LEV-induced changes in membrane potential tend to be responsive to extraneous factors that control the resting potential, such as synaptic input or neuromodulation. Furthermore, based on our simulation results, the adding effect of inhibition of $I_{K(DR)}$ under the condition in which inhibition of I_{Na} occurs, causes the termination of AP firing, reflecting the practical add-on role of LEV in Na^+ channel blocking therapy, such as phenytoin or carbamazepine (49).

Voltage-gated potassium channels have become potentially important molecular targets in modifying action potentials in various disorders including neuropsychiatry disorders, cardiology and oncology (50, 51). In addition to $K_v3.1$, there are still several components contributing to $I_{K(DR)}$, including K_v1 and 2 subunits. Although ubiquitous, in different tissues, the components of the potassium channels and their physiological function vary (52). Adequate modulation of these potassium channels including $I_{K(DR)}$ and $I_{K(erg)}$ would potentially be useful in clinical treatment (50, 53).

Taken together, from our study, the effect of LEV on $I_{K(DR)}(K_v3.1)$, could provide a therapeutic potential in treating epilepsy.

Acknowledgements: This work was partly aided by grants from the National Science Council (NSC-95-2745-B006-002-MY2 and NSC-96-2314-B-006-059), National Cheng Kung University Hospital (NCKUH-9701015) and the Program for Promoting Academic Excellence & Developing World Class Research Centers, Ministry of Education, Taiwan. The authors would like to thank technical support from Ming-Wei Lin and Ya-Jean Wang.

Conflict of interests: none declared.

REFERENCES

1. Rogawski MA. Diverse mechanisms of antiepileptic drugs in the development pipeline. *Epilepsy Res* 2006; 69: 273-294.
2. Cereghino JJ, Biton V, Abou-Khalil B, Dreifuss F, Gauer LJ, Leppik I. Levetiracetam for partial seizures: results of a double-blind, randomized clinical trial. *Neurology* 2000; 55: 236-242.
3. Carreno M. Levetiracetam. *Drugs Today (Bare)* 2007; 43: 769-794.
4. Noachtar S, Andermann E, Meyvisch P, *et al.* Levetiracetam for the treatment of idiopathic generalized epilepsy with myoclonic seizures. *Neurology* 2008; 70: 607-616.
5. Gorji A, Hohling JM, Madeja M, *et al.* Effect of levetiracetam on epileptiform discharges in human neocortical slices. *Epilepsia* 2002; 43: 1480-1487.
6. Lynch BA, Lambeng N, Nocka K, *et al.* The synaptic vesicle protein SV2A is the binding site for the antiepileptic drug levetiracetam. *Proc Natl Acad Sci USA* 2004; 101: 9861-9866.
7. Gillard M, Chatelain P, Fuks B. Binding characteristics of levetiracetam to synaptic vesicle protein 2A (SV2A) in human brain and in CHO cells expressing the human recombinant protein. *Eur J Pharmacol* 2006; 536: 102-108.
8. Lukyanetz EA, Shkryl VM, Kostyuk PG. Selective blockade of N-type calcium channels by levetiracetam. *Epilepsia* 2002; 43: 9-18.
9. Madeja M, Margineau DG, Gorji A, *et al.* Reduction of voltage-operated potassium currents by levetiracetam: a novel antiepileptic mechanism of action? *Neuropharmacology* 2003; 45: 661-671.

10. Genton P, Van Vleymen B. Piracetam and levetiracetam: close structural similarities but different pharmacological and clinical profiles. *Epileptic Disord* 2000; 2: 99-105.
11. Solntseva EI, Bukanova JV, Ostrovskaya RU, Gudasheva TA, Voronina TA, Skrebitsky VG. The effects of piracetam and its novel peptide analogue GVS-111 on neuronal voltage-gated calcium and potassium channels. *Gen Pharmacol* 1997; 29: 85-89.
12. Bukanova JV, Solntseva EI, Skrebitsky VG. Selective suppression of the slow-inactivating potassium currents by neurotrops in molluscan neurons. *Int J Neuropsychopharmacol* 2002; 5: 229-237.
13. Rehni AK, Singh N, Jindal S. Role of ATP-sensitive potassium channels in the piracetam induced blockade of opioid effects. *Indian J Exp Biol* 2007; 45: 1050-1054.
14. Wu SN, Lo YK, Chen H, Li HF, Chiang HT. Rutaecarpine-induced block of delayed rectifier K⁺ current in NG108-15 neuronal cells. *Neuropharmacology* 2001; 41: 834-843.
15. Coetzee WA, Amarillo Y, Chiu J, *et al.* Molecular diversity of K⁺ channels. *Ann N Y Acad Sci* 1999; 868: 233-285.
16. Rudy B, McBain CJ. Kv3 channels: voltage-gated K⁺ channels designed for high-frequency repetitive firing. *Trends Neurosci* 2001; 24: 517-526.
17. Tsai TY, Tsai YC, Wu SN, Liu YC. Tramadol-induced blockade of delayed rectifier potassium current in NG108-15 neuronal cells. *Eur J Pain* 2006; 10: 597-601.
18. Yokoyama S, Kawamura T, Ito Y, Hoshi N, Enomoto K, Higashida H. Potassium channels cloned from NG108-15 neuroblastoma-glioma hybrid cells. Functional expression in *Xenopus* oocytes and mammalian fibroblast cells. *Ann N Y Acad Sci* 1993; 707: 60-73.
19. Mohan DK, Molnar P, Hickman JJ. Toxin detection based on action potential shape analysis using a realistic mathematical model of differentiated NG108-15 cells. *Biosens Bioelectron* 2006; 21: 1804-1811.
20. Kawaguchi A, Asano H, Matsushima K, Wada T, Yoshida S, Ichida S. Enhancement of sodium current in NG108-15 during neural differentiation is mainly due to an increase in Na_v1.7 expression. *Neurochem Res* 2007; 32: 1469-1475.
21. Huang CW, Huang CC, Lin MW, Tsai JJ, Wu SN. The synergistic inhibitory actions of oxcarbazepine on voltage-gated sodium and potassium currents in differentiated NG108-15 neuronal cells and model neurons. *Int J Neuropsychopharmacol* 2008; 11: 597-610.
22. Sacco T, De Luca A, Tempia F. Properties and expression of Kv3 channels in cerebellar Purkinje cells. *Mol Cell Neurosci* 2006; 33: 170-179.
23. Monti B, Polazzi E, Batti L, Crochemore C, Virgili M, Contestabile A. Alpha-synuclein protects cerebellar granule neurons against 6-hydroxydopamine-induced death. *J Neurochem* 2007; 103: 518-30.
24. Wu SN, Jan CR, Li HF, Chiang HT. Characterization of inhibition by risperidone of the inwardly rectifying K(+) current in pituitary GH(3) cells. *Neuropsychopharmacology* 2000; 23: 676-689.
25. Marom S. Slow changes in the availability of voltage-gated ion channels: effects on the dynamics of excitable membranes. *J Membr Biol* 1998; 161: 105-113.
26. Liu CP, Chiang HT, Jan CR, Wu SN. Mechanism of carvedilol-induced block of delayed rectifier K⁺ current in the NG108-15 neuronal cell line. *Drug Develop Res* 2003; 58: 196-208.
27. Ermentrout GB. *Simulating, Analyzing, and Animating Dynamical System: A Guide to XPPAUT for Researchers and Students.* Society for Industrial and Applied Mathematics (SIAM). Philadelphia, 2002
28. Huang CW, Huang CC, Wu SN. Activation by zonisamide, a newer antiepileptic drug, of large-conductance calcium-activated potassium channel in differentiated hippocampal neuron-derived H19-7 cells. *J Pharmacol Exp Ther* 2007; 321: 98-106.
29. Brette R, Rudolph M, Carnevale T, *et al.* Simulation of networks of spiking neurons: a review of tools and strategies. *J Comput Neurosci* 2007; 23: 349-398.
30. Yeung SY, Thompson D, Wang Z, Fedida D, Robertson B. Modulation of Kv3 subfamily potassium currents by the sea anemone toxin BDS: significance for CNS and biophysical studies. *J Neurosci* 2005; 25:8735-8745.
31. von Rosenstiel P. Brivaracetam (UCB 34714). *Neurotherapeutics* 2007; 4: 84-87.
32. Lo YK, Chiang HT, Wu SN. Effect of arvanil (*N*-arachidonoyl-vanillyl-amine), a nonpungent anadamide-capsaicin hybrid, on ion currents in NG108-15 neuronal cells. *Biochem Pharmacol* 2003; 65: 581-591.
33. Martina M, Schultz JH, Ehmke H, Monyer H, Jonas P. Functional and molecular differences between voltage-gated K⁺ channels of fast-spiking interneurons and pyramidal neurons of rat hippocampus. *J Neurosci* 1998; 18: 8111-8125.
34. Martina M, Yao GL, Bean BP. Properties and functional role of voltage-dependent potassium channels in dendrites of rat cerebellar Purkinje neurons. *J Neurosci* 2003; 23: 5698-5707.
35. Xu M, Cao R, Xiao R, Zhu MX, Gu C. The axon-dendrite targeting of Kv3 (Shaw) channels is determined by a targeting motif that associates with the T1 domain and anykrin G. *J Neurosci* 2007; 27: 14158-14170.
36. Meador KJ, Gevins A, Loring DW, *et al.* Neuropsychological and neurophysiologic effects of carbamazepine and levetiracetam. *Neurology* 2007; 69: 2076-2084.
37. Kossoff EH, Bergey GK, Freeman JM, Vining EPG. Levetiracetam psychosis in children with epilepsy. *Epilepsia* 2001; 42: 1611-1613.
38. Baranauskas G. Ionic channel function in action potential generation: current perspective. *Mol Neurobiol* 2007; 35: 129-150.
39. Song WJ. Genes responsible for native depolarization-activated K⁺ currents in neurons. *Neurosci Res* 2002; 42: 7-14.
40. Erisir A, Lau D, Rudy B, Leonard CS. Function of specific K(+) channels in sustained high-frequency firing of fast-spiking neocortical interneurons. *J Neurophysiol* 1999; 82: 2476-2489.
41. Ho CS, Grange RW, Joho RH. Pleiotropic effects of a disrupted K⁺ channel gene: reduced body weight, impaired motor skill and muscle contraction, but no seizures. *Proc Natl Acad Sci USA* 1997; 94: 1533-1538.
42. Futatsugi Y, Riviello JJ Jr. Mechanisms of generalized absence epilepsy. *Brain Dev* 1998; 20: 75-79.
43. Joho RH, Ho CS, Marks GA. Increased gamma- and decreased delta-oscillations in a mouse deficient for a potassium channel expressed in fast-spiking interneurons. *J Neurophysiol* 1999; 82: 1855-1864.
44. Porcello DM, Ho CS, Joho RH, Huguenard JR. Resilient RTN fast spiking in Kv3.1 null mice suggests redundancy in the action potential repolarization mechanism. *J Neurophysiol* 2002; 87: 1303-1310.
45. Crowder KM, Gunther JM, Jones TA, *et al.* Abnormal neurotransmission in mice lacking synaptic vesicle protein 2A (SV2A). *Proc Natl Acad Sci USA* 1999; 96: 15268-15273.
46. Yang XF, Weisenfeld A, Rothman SM. Prolonged exposure to levetiracetam reveals a presynaptic effect on neurotransmission. *Epilepsia* 2007; 48: 1861-1869.

47. Kaminski RM, Matagne A, Leclercq K, *et al.* SV2A protein is a broad-spectrum anticonvulsant target: functional correlation between protein binding and seizure protection in models of both partial and generalized epilepsy. *Neuropharmacology* 2008; 54: 715-720.
48. Destexhe A, Rudolph M, Pare D. The high-conductance state of cortical neurons *in vivo*. *Nat Rev Neurosci* 2003; 4: 739-751.
49. Beran RG, Berkovic SF, Black AB, *et al.* Efficacy and safety of levetiracetam 1000-3000 mg/day in patients with refractory partial-onset seizures: a multicenter, open-label single-arm study. *Epilepsy Res* 2005; 63: 1-9.
50. Wang YJ, Lin MW, Lin AA, Peng H, Wu SN. Evidence for state-dependent block of DPI 201-106, a synthetic inhibitor of Na⁺ channel inactivation, on delayed-rectifier K⁺ current in pituitary tumor (GH3) cells. *J Physiol Pharmacol* 2008; 59: 409-423.
51. Teisseyre A, Duarte N, Ferreira MJ, Michalak K. Influence of the multidrug transporter inhibitors on the activity of Kv1.3 voltage-gated potassium channels. *J Physiol Pharmacol* 2009; 60: 69-76.
52. Teisseyre A, Mercik K, Mozrzymas JW. The modulatory effect of zinc ions on voltage-gated potassium currents in cultured rat hippocampal neurons is not related to Kv1.3 channels. *J Physiol Pharmacol* 2007; 58: 699-715.
53. Ridley JM, Shuba YM, James AF, Hancox JC. Modulation by testosterone of an endogenous hERG potassium channel current. *J Physiol Pharmacol* 2008; 59: 395-407.

Received: December 30, 2008

Accepted: November 6, 2009

Author's address: Dr. Sheng-Nan Wu, Department of Physiology, National Cheng Kung University Medical College, No. 1, University Road, Tainan City, 70101, Taiwan; Phone: 886-6-2353535 ext 5334; FAX: 886-6-2362780; E-mail: snwu@mail.ncku.edu.tw